ACS Sustainable Chemistry & Engineering

Research Article

pubs.acs.org/journal/ascecg

Hydrothermal Catalytic Cracking of Fatty Acids with HZSM-5

Na Mo and Phillip E. Savage*

Department of Chemical Engineering, University of Michigan, 3074 H. H. Dow Building, 2300 Hayward Street, Ann Arbor, Michigan 48109-2136, United States

Supporting Information

ABSTRACT: We explored the hydrothermal cracking of palmitic acid by HZSM-5 zeolite in a batch reactor. The major liquid products were aromatic hydrocarbons (e.g., xylenes, toluene) and alkanes (e.g., 2-methyl-pentane, heptane). The major gaseous products were CO and CO_2, but appreciable yields of propane and butane were also obtained. The effects of batch holding time, temperature, hydrogen pressure, and water density on product yields were elucidated. Total yields of gas and liquid products exceeding 90 wt % are available at reaction conditions of 400 °C, 180 min, and either with no added H_2 and a water density of 0.1 g/mL or less or with added H_2 and a water density of 0.15 g/mL. The activation energy for palmitic acid disappearance is 31 ± 1 kJ/mol. The zeolite catalyst undergoes some modest structural changes under the hydrothermal reaction conditions employed, but the catalyst can be regenerated by controlled oxidation to remove coke and calcination to restore the structure. These results demonstrate the technical feasibility of using HZSM-5 under hydrothermal conditions to produce valuable chemicals from renewable fatty acid feedstocks.

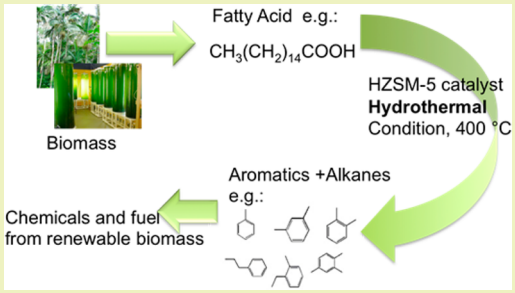

KEYWORDS: *Supercritical water, Aromatic hydrocarbons, Activation energy, Zeolite stability*

INTRODUCTION

Triglycerides and the fatty acids that they contain are attractive renewable feedstocks for hydrocarbon chemicals and fuels because they can be major components of both terrestrial and aquatic biomass (e.g., jatropha, palm, microalgae). There are several proposed chemical processes that generate aqueous streams rich in fatty acids. For example, Immer et al.[1] and Wang et al.[2] describe a fuel production process that includes hydrolysis of triglycerides and thereby produces fatty acids in water at elevated temperatures. Kusdiana and Saka[3] have proposed making biodiesel from vegetable oils by first hydrolyzing triglycerides to produce fatty acids in water. Hydrothermal liquefaction of lipid-rich algal biomass is another process that generates aqueous streams rich in fatty acids.[4] These examples show that fatty acids can be readily produced in aqueous streams. Interestingly, however, there has been little research on the hydrothermal heterogeneous catalytic conversion of fatty acids (or triglycerides) to value-added hydrocarbons for use as chemicals or fuels.

Previous work on catalytic hydrothermal conversion of fatty acids or triglycerides is limited to their gasification, deoxygenation, and hydrothermolysis. The gasification of oleic acid in supercritical water (500 °C) with Ru/Al_2O_3 and Ni/silica–alumina-generated fuel-rich gases such as hydrogen.[5] The efficacy of Pd/C, Pt/C, and even activated carbon alone for hydrothermal deoxygenation of fatty acids and triglycerides has been previously demonstrated.[6−10] These studies focused on fatty acid deoxygenation to yield the corresponding alkane as a potential component of diesel fuel. Li et al.[11] conducted catalytic hydrothermolysis of triglycerides with zinc acetate as the catalyst. They showed that this approach reduced demand for external H_2 for oxygen removal, and it produced a more diverse slate of product molecules, which was advantageous for fuel purposes.

Given the various processes that produce fatty acids in aqueous streams and the paucity of work dealing with their hydrothermal catalytic conversion to molecules other than gases or alkanes, we decided to initiate new work in this field. We selected a HZSM-5 zeolite catalyst for this work because prior work,[12−14] though not done in an aqueous phase, indicates that HZSM-5 can convert fatty acids to paraffins, olefins, and aromatic compounds that fall within the gasoline and kerosene boiling point fractions. Additionally, HZSM-5 has been shown to be useful in other biomass processing contexts,[15−18] and it has a high activity for cracking and aromatization.[19] We are unaware of any prior work on converting fatty acids into hydrocarbons using zeolites in a hydrothermal environment. This report is the first on this specific topic. Palmitic acid (PA), which is one of the most common fatty acids in nature, serves as the reactant. We identify and quantify all of the major reaction products, and we elucidate the effects of reaction time, temperature, hydrogen pressure, and water density on the yield of each. We also examine catalyst regeneration and catalyst characterization.

Special Issue: Sustainable Chemical Product and Process Engineering

Received: September 20, 2013
Revised: November 13, 2013
Published: November 15, 2013

   dx.doi.org/10.1021/sc400368n | *ACS Sustainable Chem. Eng.* 2014, 2, 88−94

MATERIALS AND METHODS

Materials. Palmitic acid with purity of 98% was acquired from ACROS Organics. The ZSM-5 was obtained in ammonium form from Zeolyst International as a white powder with a silica-to-alumina atomic ratio of 30. We calcined the fresh catalyst in air at 550 °C for 240 min to convert it to the hydrogen form HZSM-5, which increases the acidity of the zeolite and thus facilitates the cracking reactions.[20] We regenerated catalysts that had been used in an experiment by first drying them in an oven at 70 °C overnight. Next, controlled combustion (heating at 2 °C/min up to 550 °C) was carried out in air to burn off any coke. The 550 °C temperature was then maintained for 240 min to calcine the catalyst, after which the material naturally cooled to room temperature.[21,22]

Reaction Experiments. Reactions were conducted in 4 mL stainless steel Swagelok batch reactors with high-pressure valves that were connected by a length of 1/8 in. o.d. stainless steel tubing. The reactors have been described fully elsewhere.[18] A total of 150 mg of palmitic acid, 150 mg of HZSM-5, and the desired amount of water (typically 0.6 mL) were loaded into each reactor. Loading 0.6 mL of water leads to a water density of 0.15 g/mL and a pressure of 240 bar at 400 °C. These conditions exceed the critical temperature and pressure of water. Helium was added to each reactor at a pressure of 4 bar and was used as an internal standard for gas products analysis. In some cases, hydrogen was also added to the reactor. The sealed reactors were then attached to a wrist-action shaker and placed into an isothermal fluidized sand bath, which had been preheated to the desired reaction temperature for the desired reaction time. Upon removal from the sandbath, the reactors were submerged in a water bath at ambient temperature to quench the reaction.

Product Analysis. The gas-phase products were collected and analyzed with a gas chromatograph (GC) with a thermal conductivity detector (GC/TCD) and argon as the carrier gas. A Carboxen column separated the light gases such as He, H_2, CO, and C_1 and C_2 hydrocarbons, and a Porapak column separated the heavier gases including C_3 to C_5 hydrocarbons. Calibration curves were established by analyzing gas standards of known composition.

Upon completing the gas analysis, acetone was added to the reactor to recover the liquid- and solid-phase material from the reactor. The reactors were rinsed with repeated acetone washes until the total volume collected was 20 mL. The samples were transferred into a conical tube and then centrifuged at 4000 rpm for 10 min to facilitate recovery of the acetone-insoluble material (e.g., spent catalyst, coke). Acetone-soluble products were identified and quantified using Agilent 6890 GCs with a mass spectrometric (GC/MS) and a flame ionization (GC/FID) detector. Helium served as the carrier gas. We used a nonpolar HP-5 (5% phenyl-methylpolysiloxane) capillary column (50 m × 200 μm × 0.33 μm). The quantification of acetic acid (one of the identified products) and palmitic acid was performed with an Agilent 7890 GC/FID with a high polarity DBFFAP column. Calibration curves made by analyzing various standards containing reaction products in known concentrations were applied to quantify the acetone-soluble products. The Supporting Information provides more details about the chromatographic methods employed.

Molar yields of reaction products were calculated as the number of moles of product formed divided by the number of moles of palmitic acid loaded into the reactor. Many experiments were replicated, and we report standard deviations as the experimental uncertainties in these cases. The reactions produced many products in yields too low to quantify reliably on an individual basis. Because the FID is a carbon counter, however, and because the products are primarily hydrocarbons, we used the total peak area of all of the products appearing in the GC/FID chromatogram to estimate the total mass of liquid-phase products as shown below.

$$\text{Total liquid product mass} = \frac{(\text{Total mass of quantified liquid products}) \times (\text{Sum of all GC/FID product peak areas})}{\text{Sum of all quantified liquid product peak areas}}$$

We calculated the mass balance as the sum of the total product yield (including liquid and gas) and the unreacted PA yield.

RESULTS AND DISCUSSION

This section first reports results from control experiments that validate the methods used in the experiments. We next report the identities of the products generated, and how their yields changed with reaction time, temperature, hydrogen pressure, and water loading. We conclude by showing that the used catalyst can be recovered, regenerated, and used again.

Control Experiments. We completed two types of control experiments. The first involved loading PA, water, and HZSM-5 into reactors but not heating them. These experiments showed no detectable products, and an average PA recovery of 97 ± 4%. The second type of control experiments involved loading PA and water into reactors (no HZSM-5) and placing them in the sandbath for 180 min at 400 °C. This time, the average PA recovery was 66 ± 5%. The total liquid product yield was 12 ± 5 wt %. The most abundant products were xylenes, toluene, 2-methylpentane, and 2-methylhexane. The total gas product yield was 4 wt %, and the mass balance was 82%. The missing mass was presumably in the form of acetone-insolubles that were not quantified. Overall, the results indicated that no detectable amounts of products were generated without the elevated temperature, and that thermal cracking could be responsible for no more than 12 wt % liquid product yield at 400 °C and 180 min, the most severe conditions examined in this investigation.

Reaction Products. Figure S1 of the Supporting Information shows a representative total ion chromatogram for the reaction products appearing from HZSM-5-catalyzed palmitic acid cracking in supercritical water. The major products are the aromatic compounds toluene, 1,4-dimethylbenzene (*p*-xylene), 1-ethyl-2-methyl-benzene, and 1,2,4-trimethylbenzene. The other xylene isomers and propylbenzene are also present. Toluene, *p*-xylene, 1-ethyl-2-methyl-benzene, and 1,2,4-trimethylbenzene were major products from cracking oleic acid at 400 °C with HZSM-5, but without water.[12] Thus, it appears that the presence of water in the present hydrothermal conversion experiments did not affect the types of major products generated from cracking fatty acids.

Some of the aromatic hydrocarbons in the product mixture are chemicals produced in very large volumes worldwide, often by the catalytic reforming of naphtha in a petroleum refinery.[23] They have various uses in the chemical industry. For example, *p*-xylene is a precursor of terephthalic acid, which is a monomer used to make polyethylene terephthalate, a plastic widely used in the production of fibers and beverage bottles.

In addition to the aromatic products, 2-methyl-pentane, butanal, acetic acid, 2-methyl-hexane, 2-pentanone, heptane, and 4-methyl-heptane are also reaction products. The alkanes can be used as a fuel, and heptane is a raw material for manufacture of paints and coatings. Acetic acid is a key reactant in producing vinyl acetate monomer.

The gaseous products from cracking PA at 400 °C with HZSM-5 were C_1 to C_5 alkanes, CO, and CO_2. This product

dx.doi.org/10.1021/sc400368n | ACS Sustainable Chem. Eng. 2014, 2, 88−94

Table 1. Molar Yields of Major Products from Palmitic Acid Cracking Over HZSM-5 at Different Reaction Times, Temperature, and Water Density

run number	1	2	3	4	5	6	7	8	9	10	11
reaction temperature (°C)	400	400	400	400	400	400	400	400	400	300	200
reaction time (min)	25	35	45	60	90	180	180	180	180	180	180
water loading (mL)	0.6	0.6	0.6	0.6	0.6	0.6	0.4	0.2	0	0.6	0.6
auto generated pressure (bar)	240	240	240	240	240	240	200	125	NA	86	15
water density (g/mL)	0.15	0.15	0.15	0.15	0.15	0.15	0.1	0.05	0	NA	NA
product yield (mol/mol PA)											
2-methyl-pentane	0.023 ± 0.016	0.040 ± 0.038	0.068 ± 0.027	0.078 ± 0.032	0.11 ± 0.02	0.062 ± 0.053	0.047 ± 0.008	0.028 ± 0.009	ND	ND	ND
butanal	0.019 ± 0.006	0.029 ± 0.014	0.017 ± 0.006	0.056 ± 0.025	0.037 ± 0.003	0.051 ± 0.022	0.032 ± 0.004	0.015 ± 0.008	0.0045 ± 0.0063	0.0023	ND
2-methyl-hexane	0.0045 ± 0.0089	0.020 ± 0.014	0.016 ± 0.011	0.020 ± 0.002	0.042 ± 0.010	0.026 ± 0.008	0.025 ± 0.008	0.0030 ± 0.0059	ND	ND	ND
2-pentanone	0.0098 ± 0.0048	0.014 ± 0.005	0.014 ± 0.003	0.0096 ± 0.0074	0.020 ± 0.009	0.0052 ± 0.0021	0.012 ± 0.003	0.028 ± 0.007	0.092 ± 0.072	ND	ND
heptane	0.0055 ± 0.0042	0.0089 ± 0.0050	0.011 ± 0.003	0.016 ± 0.017	0.015 ± 0.013	0.0089 ± 0.0023	0.012 ± 0.005	0.0049 ± 0.0057	ND	ND	ND
4-methyl-heptane	0.0012 ± 0.0024	0.0049 ± 0.0030	0.0063 ± 0.0012	0.0041 ± 0.0028	0.0048 ± 0.0002	0.0025 ± 0.0028	0.0036 ± 0.0033	ND	ND	ND	ND
toluene	0.090 ± 0.023	0.093 ± 0.050	0.082 ± 0.031	0.11 ± 0.05	0.187 ± 0.003	0.22 ± 0.03	0.36 ± 0.03	0.47 ± 0.05	0.53 ± 0.06	ND	ND
xylene	0.25 ± 0.07	0.29 ± 0.14	0.29 ± 0.12	0.28 ± 0.02	0.44 ± 0.04	0.49 ± 0.08	0.68 ± 0.09	0.71 ± 0.09	0.62 ± 0.08	0.03	0.069
propyl-benzene	0.011 ± 0.007	0.010 ± 0.007	0.0068 ± 0.008	0.015 ± 0.013	0.0170 ± 0.0001	0.034 ± 0.030	0.10 ± 0.02	0.076 ± 0.021	0.029 ± 0.002	ND	ND
2-ethyl-toluene	0.024 ± 0.010	0.029 ± 0.014	0.030 ± 0.018	0.025 ± 0.009	0.028 ± 0.004	0.036 ± 0.012	0.024 ± 0.006	0.023 ± 0.004	0.011 ± 0.002	ND	ND
1,2,4-trimethylbenzene	0.011 ± 0.008	0.015 ± 0.009	0.015 ± 0.012	0.018 ± 0.004	0.0302 ± 0.0006	0.029 ± 0.008	0.045 ± 0.006	0.050 ± 0.008	0.050 ± 0.010	ND	ND
acetic acid	ND	ND	ND	0.015 ± 0.027	0.0016 ± 0.0002	0.11 ± 0.04	0.043 ± 0.034	0.023 ± 0.005	0.0028 ± 0.0001	0.00073	ND
H_2	NA	NA	NA	0.013 ± 0.016	NA	0.085 ± 0.023	0.073 ± 0.016	0.063 ± 0.013	0.16 ± 0.01	NA	NA
CO	NA	NA	NA	0.14 ± 0.04	NA	0.126 ± 0.005	0.14 ± 0.08	0.14 ± 0.02	0.182 ± 0.003	NA	NA
CH_4	NA	NA	NA	0.038 ± 0.025	NA	0.020 ± 0.010	0.027 ± 0.003	0.038 ± 0.031	0.37 ± 0.08	NA	NA
CO_2	NA	NA	NA	0.23 ± 0.09	NA	0.30 ± 0.07	0.47 ± 0.16	0.37 ± 0.04	0.210 ± 0.001	NA	NA
C_2H_4	NA	NA	NA	0.0032 ± 0.0046	NA	0.090 ± 0.015	0.042 ± 0.049	0.10 ± 0.08	0.45 ± 0.23	NA	NA
C_2H_6	NA	NA	NA	0.021 ± 0.015	NA	0.0155 ± 0.0006	0.025 ± 0.006	0.044 ± 0.027	0.39 ± 0.08	NA	NA
C_3H_8	NA	NA	NA	0.24 ± 0.15	NA	0.13 ± 0.03	0.21 ± 0.06	0.27 ± 0.22	0.80 ± 0.10	NA	NA
n-C_4H_{10}	NA	NA	NA	0.25 ± 0.16	NA	0.10 ± 0.04	0.13 ± 0.06	0.097 ± 0.039	0.068 ± 0.013	NA	NA
i-C_4H_{10}	NA	NA	NA	0.10 ± 0.04	NA	0.051 ± 0.025	0.068 ± 0.037	0.060 ± 0.039	0.062 ± 0.008	NA	NA
C_5H_{12}	NA	NA	NA	0.050 ± 0.044	NA	0.037 ± 0.020	0.034 ± 0.023	0.025 ± 0.015	ND	NA	NA
total liquid products (mg/mg PA)	0.31 ± 0.13	0.41 ± 0.19	0.40 ± 0.15	0.39 ± 0.03	0.57 ± 0.06	0.59 ± 0.12	0.73 ± 0.09	0.71 ± 0.08	0.65 ± 0.04	0.038	0.049
total gas products (mg/mg PA)	NA	NA	NA	0.11 ± 0.01	NA	0.16 ± 0.04	0.20 ± 0.02	0.22 ± 0.07	0.34 ± 0.03	NA	NA
total yield (wt%)	NA	NA	NA	50 ± 5.5	NA	76 ± 13	92 ± 7.7	93 ± 6.5	99 ± 7.0	NA	NA
PA conversion (%)	43	49	50	72 ± 13	76	95 ± 4.0	97 ± 1.8	99 ± 0.21	99 ± 0.03	52	25
mass balance (wt %)	NA	NA	NA	78 ± 7.6	NA	81 ± 11	95 ± 9.5	94 ± 6.7	99 ± 7.0	NA	NA

dx.doi.org/10.1021/sc400368n | ACS Sustainable Chem. Eng. 2014, 2, 88−94

slate is largely consistent with previous reports on fatty acid cracking with zeolites (though not in water).[12,13] The hydrocarbon gases are useful as a fuel in a biorefinery, and they also have uses as chemical feedstocks. Methane is a feedstock for producing hydrogen via steam reforming. Ethane is used in producing hydrogen and ethylene. *n*- and *i*-Butane can be blended as components of gasoline to give it a more desirable vapor pressure.[24] It is clear that hydrothermal catalytic conversion of palmitic acid over HZSM-5 produces molecules that are useful as chemicals and as components in liquid transportation fuels.

Effect of Time and Temperature on Product Yields. We conducted experiments at 400 °C and several different reaction times to explore the influence of this process variable on the product yields. We also did experiments for 180 min at 200, 300, and 400 °C to explore the effect of temperature on this hydrothermal catalytic conversion.

Table 1 (Runs 1−6) lists the molar yields of the identified products from the reaction at 400 °C and at the different batch holding times explored. The most abundant products at short times are 2-methyl-pentane, butanal, 2-ethyltoluene, toluene, and xylenes. The molar yields of 2-methyl-pentane and butanal reach maxima at 60 and 90 min, respectively, and then decrease. The change in yield of 2-ethyltoluene with time is less than the experimental uncertainty, so we consider this yield to be essentially time invariant. In contrast, the yields of toluene and xylenes, shown in Figure 1, increase steadily with

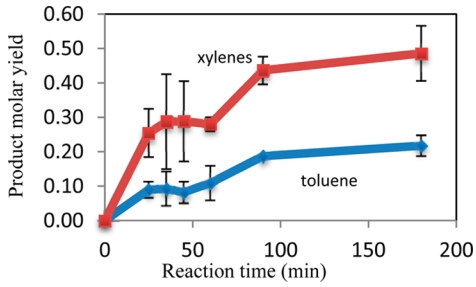

Figure 1. Temporal variation of toluene and xylenes molar yields at 400 °C.

time and reach 22% and 49%, respectively, at 180 min. These are the major products. Acetic acid is below detection limits through 45 min, but its yield increases to >10% at 180 min. The conversion of palmitic acid increased with time and reached 95% at 180 min. The total liquid product yield reached 59 wt % at 180 min.

The final row in Table 1 shows the overall mass balance for the two reaction times (60 and 180 min) at 400 °C where gas products were quantified. The mass balance is 81 ± 11% for the 180 min reaction and 78 ± 8% for the 60 min reaction. One possible contributor to the incomplete mass balance is the generation of coke during the reaction, which is common during hydrocarbon processing with zeolites.[25] Coke formation during these experiments seems likely given the color change observed for the catalyst after each experiment. The catalyst recovered from the runs at short times, such as 25 and 35 min, retained its original white color. The catalysts recovered from runs at 45, 60, and 90 min were different shades of gray. The color turned into a darker gray for the 180 min reactions. It is likely that the amount of coke increased with increasing reaction time and that these higher coke contents corresponded to the increasingly dark color of the remaining solids.

Runs 6, 10, and 11 in Table 1 show the effect of temperature on the product yields for a 180 min batch holding time. The PA conversion at 200 °C was only 25%, and xylenes were the only products present in sufficiently high yield to quantify. At 300 °C, the conversion was 52%, and some oxygenates appeared along with xylenes. At 400 °C, the complete product slate illustrated in Figure S1 of the Suppporting Information appeared. These results indicate that a reaction temperature around 400 °C is required to generate appreciable product yields from the hydrothermal catalytic cracking of palmitic acid over HZSM-5.

We used the PA conversions in Table 1 to calculate the rate constant for PA disappearance at each temperature. The conversion data at 400 °C are consistent with first-order kinetics, and the rate constant was 2.6×10^{-4} s^{-1} ± 3.8×10^{-6} s^{-1}. The rate constants at 200 and 300 °C are 2.6×10^{-5} s^{-1} and 6.9×10^{-5} s^{-1}, respectively. The activation energy for PA disappearance was determined to be 31 ± 1 kJ/mol. Comparing this value to typical activation energies for diffusion in HZSM-5[26] indicates that the reaction is probably diffusion limited under the conditions used herein. The Arrhenius pre-exponential factor was 5.6×10^{-2} ± 2.2×10^{-3} s^{-1} or 1.5×10^{-3} ± 5.9×10^{-5} L $gcat^{-1}$ s^{-1}.

Effect of Water Density. The literature indicates that the water density can influence reaction rates and product selectivities for reactions at supercritical temperatures.[27] Therefore, we desired to discover the effect of the water density on this reaction system.

Runs 6−9 in Table 1 show the product yields obtained from experiments at 400 °C and 180 min with water densities of 0, 0.05, 0.10, and 0.15 g/mL. In the absence of water (run 9), aromatics dominate the product spectrum, with toluene and xylenes being the major products. Only one non-aromatic liquid-phase product, 2-pentanone, is present in a yield exceeding 1%. Hydrocarbons dominate the gaseous products, as the yield of each C_1 to C_3 hydrocarbon exceeds that of CO or CO_2. The palmitic acid conversion is essentially complete and about one-third of the initial mass appears as gaseous products, while the balance forms liquid-phase products.

The yields of the various products respond differently to the presence of water and to its density. The yield of acetic acid, for example, increases nearly 50-fold as the water density increased from zero to 0.15 g/mL. Other products showing consistently increasing yields (though less dramatic than acetic acid) with increasing water density include 2-methyl-pentane, butanal, 2-methyl hexane, 2-ethyl toluene, and pentane. In contrast to the behavior of the products just listed, the yields of other products either consistently decrease with increasing water density or exhibit a maximum yield at some intermediate density. Toluene, trimethyl-benzene, 2-pentanone, CO, methane, ethane, and propane are examples of the former, and heptane, 4-methyl heptane, xylenes, and propyl benzene, butanes, and CO_2 are examples of the latter. The reason(s) for these changes in product selectivity with changing water density is not clear at present, but it is clear that the water density can be used as a process variable to direct the system to favor one product over another.

As shown in Table 1, methane, ethylene, ethane, and propane form in much higher yields when there is no water in the reactor (run 9). In contrast, the yields of *i*- and *n*-butane and *n*-pentane are about the same (given the experimental uncertainties) with or without water. The presence of water reduces the yield of carbon monoxide and increases the yield of

dx.doi.org/10.1021/sc400368n | ACS Sustainable Chem. Eng. 2014, 2, 88−94

carbon dioxide. This outcome is consistent with the water gas shift reaction converting some of the CO produced into CO_2. HZSM-5 is not necessarily a good water gas shift catalyst, but this reaction can occur readily in supercritical water even in the absence of a catalyst.[28]

Effect of Hydrogen. Hydrogen is often used with zeolite Y or zeolite Beta (with or without metal) for hydrocracking reactions.[29] There is also precedent for using hydrogen to facilitate cracking reactions with HZSM-5.[30] More recently, high-pressure hydrogen was used with a zeolite catalyst for upgrading algal bio-oil, which contains a significant amount of fatty acids.[16,18] Therefore, we deemed it relevant to determine the effect of added hydrogen on hydrothermal treatment of fatty acids with HZSM-5. We conducted experiments both with and without hydrogen but at otherwise identical reaction conditions. We added 4, 25, and 50 bar (at room temperature) of hydrogen pressure to the reactor, which results in mole ratios of hydrogen to palmitic acid of roughly 0.5:1, 3:1, and 6:1, respectively.

Table S1 of the Supporting Information shows all of the product yields, PA conversions, and mass balances, and Figure 2

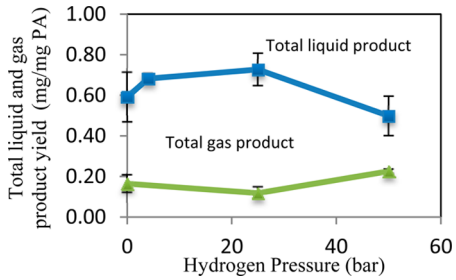

Figure 2. Effect of hydrogen pressure on total mass yields of liquid and gas products (180 min, 400 °C, 0.15 g/mL water density).

displays selected results. The PA conversion, yields of the major products, and total yields of liquid and gas products were largely insensitive to the H_2 loading for H_2 pressures up to 25 bar. When the hydrogen loading increased from 25 to 50 bar, however, the total liquid product yield dropped from 73 to 50 wt %, while the total gas product yield climbed from 12 to 23 wt %. The yields of ethane, propane, butanes, and pentane more than doubled. On the other hand, the yields of toluene and xylenes decreased noticeably. The absence of ethylene at the highest H_2 pressure is consistent with it being more readily hydrogenated as more hydrogen is added to the system. Likewise, the reduced yields of aromatics are consistent with the additional hydrogen making the dehydrocyclization reactions more difficult. These results show that moderate H_2 pressures do not adversely impact the total product yields but they do shift the product distribution to more gaseous products.

Catalyst Reuse. Zeolites undergo coking reactions during hydrocarbon processing that can reduce the catalyst activity.[31] Additionally, some zeolites are unstable under certain hydrothermal conditions.[32] Given this background, we desired to determine whether HZSM-5 could be reused for fatty acid cracking in a hydrothermal environment. We first conducted an experiment wherein the catalyst used in one reaction (400 °C, 0.15 g/mL water density, 180 min) was collected, dried in an oven at 70 °C overnight, and then reused in a second run at the same conditions. The total product yield (liquid plus gas) was 76% with the fresh catalyst, but it dropped to only 2% with the once-used catalyst. It is clear that catalyst deactivation occurred either during the hydrothermal reaction or during the hydrothermal heating/cooling experienced by the catalyst. Regardless of where or how the deactivation occurs, the issue of practical significance becomes that of catalyst regeneration. We investigated catalyst regeneration by performing a controlled oxidation of the used catalyst to burn off any coke and then subjecting that material to a calcination step as described in the experimental section.

Figures 3 and 4 show the yields of selected products from experiments with fresh catalyst (cycle 1), with catalyst that had

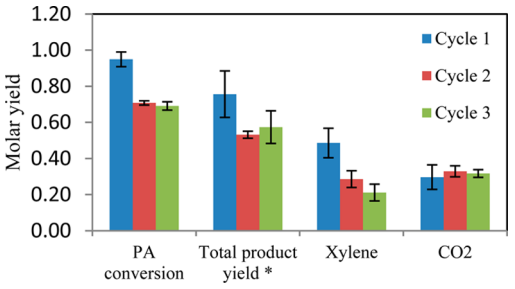

Figure 3. Effect of catalyst regeneration and reuse on palmitic acid conversion, molar yield of xylene and CO_2, and total *mass yield (not molar yield) of the liquid and gas products (180 min, 400 °C, 0.15 g/mL water density).

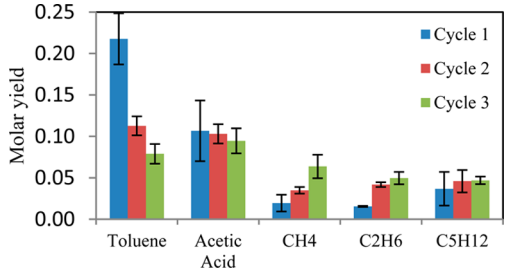

Figure 4. Effect of catalyst regeneration and reuse on molar yields of toluene, acetic acid, methane, ethane, and pentane at 180 min, 400 °C, and 0.15 g/mL water density.

been used and regenerated once (cycle 2) and with catalyst that had been used twice and regenerated twice (cycle 3). Table S2 of the Supporting Information provides the details for all of the reaction products. As indicated in Figure 3, the total product yield decreased from 76 ± 13 wt % with the fresh catalyst to 53 ± 1.9 wt % upon its second use. This irreversible deactivation in the first reaction−regeneration cycle is typical of HZSM-5 zeolites, and one reason is the loss of a certain fraction of the Brønsted strong acid sites in hot compressed water, which are required for the cracking reactions.[31] Figure 3 also shows that the total product yields are about the same for the second and third uses of the catalyst, which suggests that this hydrothermal reaction−regeneration process might be effective for hydrothermal conversion of fatty acids to hydrocarbons with value as fuels or chemicals.

Figures 3 and 4 show that the molar yields of the major products (toluene and xylenes) decrease with each reuse and regeneration of the catalyst, but appreciable yields of these desirable aromatic products are still obtained. Interestingly, the yield of acetic acid is unaffected by the reuse and regeneration of the catalyst (Figure 4). It seems that the aromatic compounds and acetic acid might be formed in two different paths,

dx.doi.org/10.1021/sc400368n | ACS Sustainable Chem. Eng. 2014, 2, 88−94

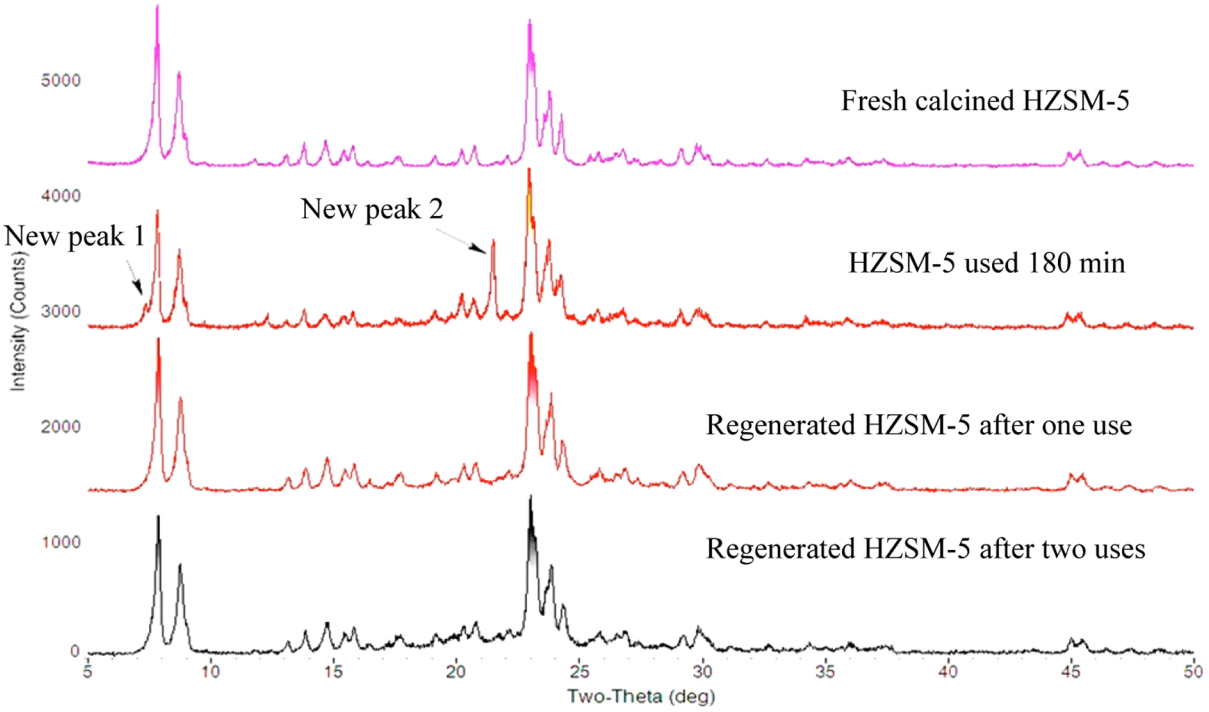

Figure 5. X-ray powder diffraction spectra for fresh calcined HZSM-5, HZSM-5 used after a 180 min reaction at 400 °C, and regenerated HZSM-5 after one and two uses.

with one being insensitive to reuse of the catalyst. CO_2 and *n*-pentane also have similar yields with fresh and regenerated catalyst. The yields of methane and ethane slightly increased when using regenerated catalyst, as indicated in Figure 4.

Catalyst Characterization. Ravenelle et al. have reported that treatment in hot liquid water (150 and 200 °C) transforms zeolite Y into an amorphous material. In contrast, HZSM-5 was not modified under the same conditions. They pointed out that the main degradation mechanism is probably hydrolysis of the siloxane bonds (Si−O−Si) as opposed to dealumination, which dominates under steaming conditions.[32] No work has been done on the stability of HZSM-5 in supercritical water at 400 °C, to the best of our knowledge.

To better understand the hydrothermal stability of HZSM-5 under the present reaction conditions, we used X-ray powder diffraction (XRD) to examine the fresh catalyst and samples of HZSM-5 recovered from reactors after use for 180 min. The XRD analysis gives information about the bulk structure of the material and the type of chemical bonds in the catalyst crystal. Figure 5 shows the XRD spectra. The fresh catalyst exhibits the XRD spectrum one expects for HZSM-5.[32] Two new peaks appear in the XRD spectrum of the HZSM-5 that was used for a 180 min reaction, however. We were unable to identify the first new peak at 7.3°, but the second new peak at 21.48° corresponds to cristobalite high-SiO_2. Though the hydrothermal reaction conditions induced some changes in the HZSM-5, the persistence of the other characteristic peaks verifies that the HZSM-5 retained its major structural elements during the reaction.

Since the hydrothermal reaction changed a portion of the catalyst structure, we analyzed the regenerated catalyst to learn whether the regeneration process restores the catalyst to its original structure. Figure 5 shows that all of the characteristic peaks in the XRD spectrum for fresh HZSM-5 also appear for the once- and twice-regenerated material. This outcome indicates that the bulk structure of HZSM-5 after regeneration is the same as the bulk structure of the fresh HZSM-5 that has been calcined. Also, after the regeneration process, the two new peaks that appeared for the used catalyst vanish.

CONCLUSION

The results presented herein demonstrate that hydrocarbon molecules such as aromatics, alkanes, and fuel gases can be produced from palmitic acid via hydrothermal catalytic cracking over HZSM-5. This work broadens to aromatics the suite of hydrocarbon molecules available via hydrothermal catalytic treatment of fatty acids. Previous work has demonstrated the decarboxylation of fatty acids to produce long-chain alkanes.[7]

Though the catalyst loses its activity after use, it can be regenerated via controlled oxidation and calcination. The XRD patterns for the fresh and regenerated catalysts were indistinguishable, which suggests that the regeneration procedure restores the bulk structure of HZSM-5. We demonstrated three consecutive uses of the same catalyst material. Thus, hydrothermal catalytic cracking might be useful for converting aqueous streams of fatty acids into molecules with applications as chemicals and fuels.

The reaction temperature, batch holding time, and water density all influence the product yields. On the other hand, added hydrogen has no significant effect on the product yields until the amount added is large enough (50 bar at room temperature) to inhibit the dehydrocyclization reactions that produce the aromatic products. The highest yield of liquid-phase products (73 ± 9 wt %) occurred at 400 °C, 180 min, a water density of 0.1 g/mL, and in the absence of added H_2. The disappearance of palmitic acid at 400 °C was consistent with first-order kinetics, and the activation energy of 31 kJ/mol suggests that the reaction is diffusion limited at the conditions studied.

dx.doi.org/10.1021/sc400368n | *ACS Sustainable Chem. Eng.* 2014, 2, 88−94

■ ASSOCIATED CONTENT

Supporting Information

Details about the analytical methods. Table S1 shows the effect of hydrogen on product yields. Table S2 shows the effect of catalyst regeneration and reuse on product yields for reaction at 150 mg of PA, 150 mg of HZSM-5 at 400 °C, 3 h. Both tables include individual product yields, total product yield, PA conversion, and mass balance. Figure S1 shows a typical total ion chromatogram of the reaction products with several of the product peaks marked with their chemical structures. This material is available free of charge via the Internet at http://pubs.acs.org.

■ AUTHOR INFORMATION

Corresponding Author

*E-mail: psavage@umich.edu. Tel: +1 734-764-3386. Fax: +1 734-763-0459.

Notes

The authors declare no competing financial interest.

■ ACKNOWLEDGMENTS

We thank Ryan Hockstad for performing some of the experiments and Thomas Yeh for assistance with the catalyst characterization. We gratefully acknowledge financial support from the National Science Foundation (CBET-1133439).

■ REFERENCES

(1) Immer, J. G.; Kelly, M. J.; Lamb, H. H. Catalytic reaction pathways in liquid-phase deoxygenation of C18 free fatty acids. *Appl. Catal., A* **2010**, *375* (1), 134−139.

(2) Wang, W. C.; Thapaliya, N.; Campos, A.; Stikeleather, L. F.; Roberts, W. L. Hydrocarbon fuels from vegetable oils via hydrolysis and thermo-catalytic decarboxylation. *Fuel* **2012**, *95*, 622−629.

(3) Kusdiana, D.; Saka, S. Effects of water on biodiesel fuel production by supercritical methanol treatment. *Bioresour. Technol.* **2004**, *91* (3), 289−295.

(4) Brown, T. M.; Duan, P.; Savage, P. E. Hydrothermal liquefaction and gasification of Nannochloropsis sp. *Energy Fuels* **2010**, *24* (6), 3639−3646.

(5) Youssef, E. A.; Nakhla, G.; Charpentier, P. A. Oleic acid gasification over supported metal catalysts in supercritical water: Hydrogen production and product distribution. *Int. J. Hydrogen Energy* **2011**, *36* (8), 4830−4842.

(6) Yang, C.; Nie, R.; Fu, J.; Hou, Z.; Lu, X. Production of aviation fuel via catalytic hydrothermal decarboxylation of fatty acids in microalgae oil. *Bioresour. Technol.* **2013**, *146*, 569−573.

(7) Fu, J.; Lu, X.; Savage, P. E. Catalytic hydrothermal deoxygenation of palmitic acid. *Energy Environ. Sci.* **2010**, *3* (3), 311−317.

(8) Fu, J.; Lu, X.; Savage, P. E. Hydrothermal decarboxylation and hydrogenation of fatty acids over Pt/C. *ChemSusChem* **2011**, *4* (4), 481−486.

(9) Fu, J.; Shi, F.; Thompson, L. T., Jr; Lu, X.; Savage, P. E. Activated carbons for hydrothermal decarboxylation of fatty acids. *ACS Catal.* **2011**, *1* (3), 227−231.

(10) Idesh, S.; Kudo, S.; Norinaga, K.; Hayashi, J. I. Catalytic hydrothermal reforming of jatropha oil in subcritical water for the production of green fuels: Characteristics of reactions over Pt and Ni catalysts. *Energy Fuels* **2013**, *27* (8), 4796−4803.

(11) Li, L.; Coppola, E.; Rine, J.; Miller, J. L.; Walker, D. Catalytic hydrothermal conversion of triglycerides to non-ester biofuels. *Energy Fuels* **2010**, *24* (2), 1305−1315.

(12) Benson, T. J.; Hernandez, R.; White, M. G.; French, W. T.; Alley, E. E.; Holmes, W. E.; Thompson, B. Heterogeneous cracking of an unsaturated fatty acid and reaction intermediates on H+ ZSM-5 catalyst. *Clean: Soil, Air, Water* **2008**, *36* (8), 652−656.

(13) Bielansky, P.; Weinert, A.; Schönberger, C.; Reichhold, A. Gasoline and gaseous hydrocarbons from fatty acids via catalytic cracking. *Biomass Convers. Biorefin.* **2012**, *2* (1), 53−61.

(14) Ooi, Y. S.; Zakaria, R.; Mohamed, A. R.; Bhatia, S. Catalytic conversion of fatty acids mixture to liquid fuel and chemicals over composite microporous/mesoporous catalysts. *Energy fuels* **2005**, *19* (3), 736−743.

(15) Cheng, Y. T.; Wang, Z.; Gilbert, C. J.; Fan, W.; Huber, G. W. Production of p-xylene from biomass by catalytic fast pyrolysis using ZSM-5 catalysts with reduced pore openings. *Angew. Chem., Int. Ed.* **2012**, *51* (44), 11097−11100.

(16) Li, Z.; Savage, P. E. Feedstocks for fuels and chemicals from algae: Treatment of crude bio-oil over HZSM-5. *Algal Res.* **2013**, *2* (2), 154−163.

(17) Milne, T.; Evans, R. J.; Nagle, N. Catalytic conversion of microalgae and vegetable oils to premium gasoline, with shape-selective zeolites. *Biomass* **1990**, *21* (3), 219−232.

(18) Duan, P.; Savage, P. E. Upgrading of crude algal bio-oil in supercritical water. *Bioresour. Technol.* **2011**, *102* (2), 1899−1906.

(19) Lestari, S.; Mäki-Arvela, P.; Beltramini, J.; Lu, G. Q.; Murzin, D. Y. Transforming triglycerides and fatty acids into biofuels. *ChemSusChem* **2009**, *2* (12), 1109−1119.

(20) Pan, P.; Hu, C.; Yang, W.; Li, Y.; Dong, L.; Zhu, L.; Tong, D.; Qing, R.; Fan, Y. The direct pyrolysis and catalytic pyrolysis of *Nannochloropsis* sp. residue for renewable bio-oils. *Bioresour. Technol.* **2010**, *101* (12), 4593−4599.

(21) Zhao, C.; Lercher, J. A. Upgrading pyrolysis oil over Ni/HZSM-5 by cascade reactions. *Angew. Chem.* **2012**, *124* (24), 6037−6042.

(22) Vispute, T. P.; Zhang, H.; Sanna, A.; Xiao, R.; Huber, G. W. Renewable chemical commodity feedstocks from integrated catalytic processing of pyrolysis oils. *Science* **2010**, *330* (6008), 1222−1227.

(23) Santos, K. A. O.; Neto, A. D.; Moura, M. C. P. A.; Dantas, T. C. Separation of xylene isomers through adsorption on microporous materials: A review. *Braz. J. Pet. Gas* **2011**, *5* (4), 255−268.

(24) Gary, J. H.; Handwerk, G. E. *Petroleum Refining*; CRC Press: New York, 2001.

(25) Jacobs, P. A., Flanigen, E. M., Jansen, J. C., van Bekkum, H. *Introduction to Zeolite Science and Practice*, 2 nd ed,; Elsevier Science: Amsterdam, 2001.

(26) Xiao, J.; Wei, J. Diffusion Mechanism of Hydrocarbons in Zeolites − II. Analysis of Experimental Observations. *Chem. Eng. Sci.* **1992**, *47* (5), 1143−1159.

(27) Duan, P.; Savage, P. E. Catalytic hydrothermal hydrodenitrogenation of pyridine. *Appl. Catal., B* **2011**, *108*, 54−60.

(28) Rice, S. F.; Steeper, R. R.; Aiken, J. D. Water density effects on homogeneous water-gas shift reaction kinetics. *J. Phys. Chem. A* **1998**, *102* (16), 2673−2678.

(29) Zhang, X.; Guo, Q.; Qin, B.; Zhang, Z.; Ling, F.; Sun, W.; Li, R. Structural features of binary microporous zeolite composite Y-Beta and its hydrocracking performance. *Catal. Today* **2010**, *149* (1), 212−217.

(30) Meusinger, J.; Corma, A. Activation of hydrogen on zeolites: Kinetics and mechanism of n-heptane cracking on H-ZSM-5 zeolites under high hydrogen pressure. *J. Catal.* **1995**, *152* (1), 189−197.

(31) Valle, B.; Gayubo, A. G.; Alonso, A.; Aguayo, A. T.; Bilbao, J. Hydrothermally stable HZSM-5 zeolite catalysts for the transformation of crude bio-oil into hydrocarbons. *Appl. Catal., B* **2010**, *100* (1), 318−327.

(32) Ravenelle, R. M.; Schüβler, F.; D'Amico, A.; Danilina, N.; Van Bokhoven, J. A.; Lercher, J. A.; Jones, C. W.; Sievers, C. Stability of zeolites in hot liquid water. *J. Phys. Chem. C* **2010**, *114* (46), 19582−19595.